Finite Elements Solution of the Fiber-Matrix Interface Crack: Effects of Mesh Refinement and Domain Size

L. Di Stasio[1,2], Z. Ayadi[1], J. Varna[2]

[1] EEIGM, Université de Lorraine, Nancy, France

[2] Division of Materials Science, Luleå University of Technology, Luleå, Sweden

DocMASE Summer School, Sarrebrücken (DE) - Nancy (FR), September 11 - 15, 2017

Outline

- The Fiber-Matrix Interface Problem in Fiber Reinforced Polymer Laminates
- Objectives & Approach
- Micromechanical modeling
- Preliminary Results & Perspectives
- Conclusions & Outlook
- Appendices & References

The Fiber-Matrix Interface Problem in FRPC

Intralaminar Transverse Cracking

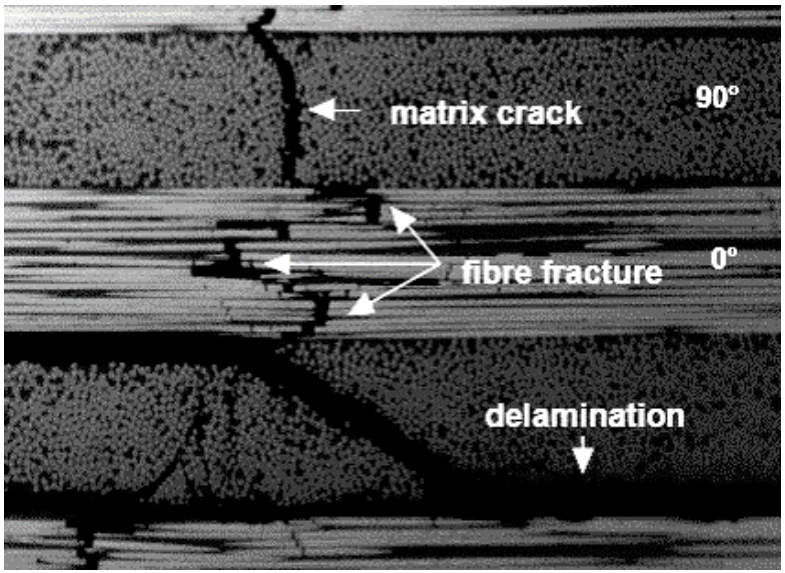

(a) By Dr. R. Olsson, Swerea, SE.

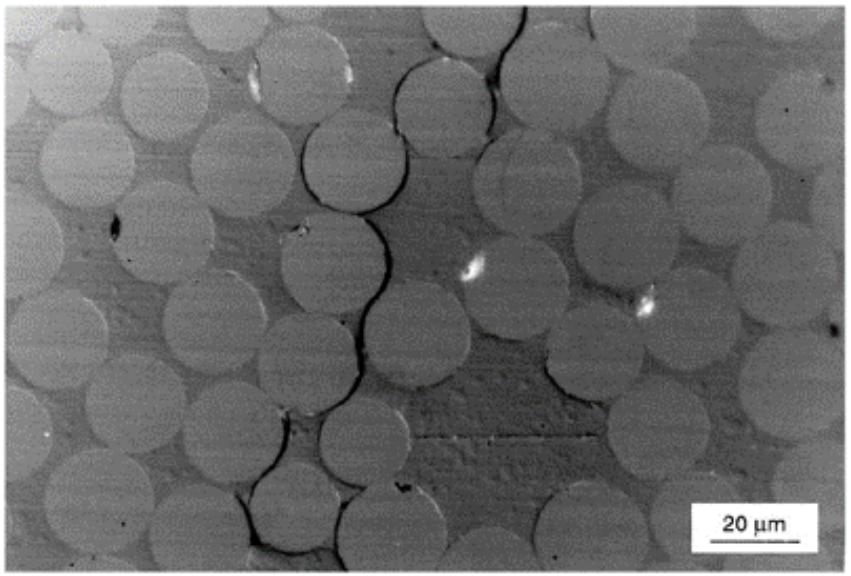

(b) By Prof. Dr. E. K. Gamstedt, KTH, SE.

For a visual definition of intralaminar transverse cracking.

The Thin Ply Effect

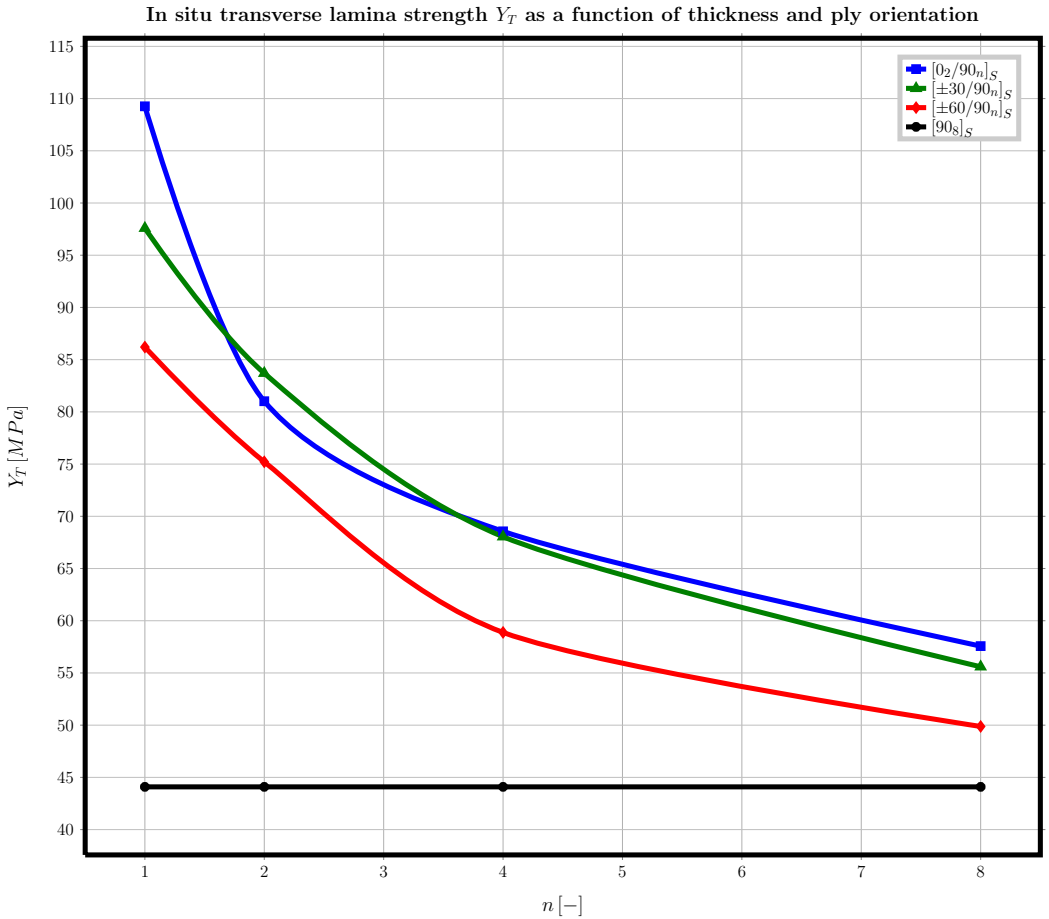

Measurements of in-situ transverse strength from D. L. Flaggs & M. H. Kural, 1982 [1].

↘ OBJECTIVES & APPROACH

Objectives & Approach

Objectives

- Investigate the influence of volume fraction, thin ply thickness and bounding plies' thicknesses on crack initiation
- To infere a relationship like

$$G_{*c} = G_{*c}\left(\theta_{debond}, \Delta\theta_{debond}, E_{(..)}, \nu_{(..)}, G_{()}, VF_f, t_{ply}, \frac{t_{ply}}{t_{bounding\ plies}}\right)$$

Approach

- Design and categorization of different Representative Volume Elements (RVEs)
- Automated generation of RVEs geometry and FEM model
- Finite Element Simulation (in Abaqus)

MICROMECHANICAL MODELING

From macro to micro

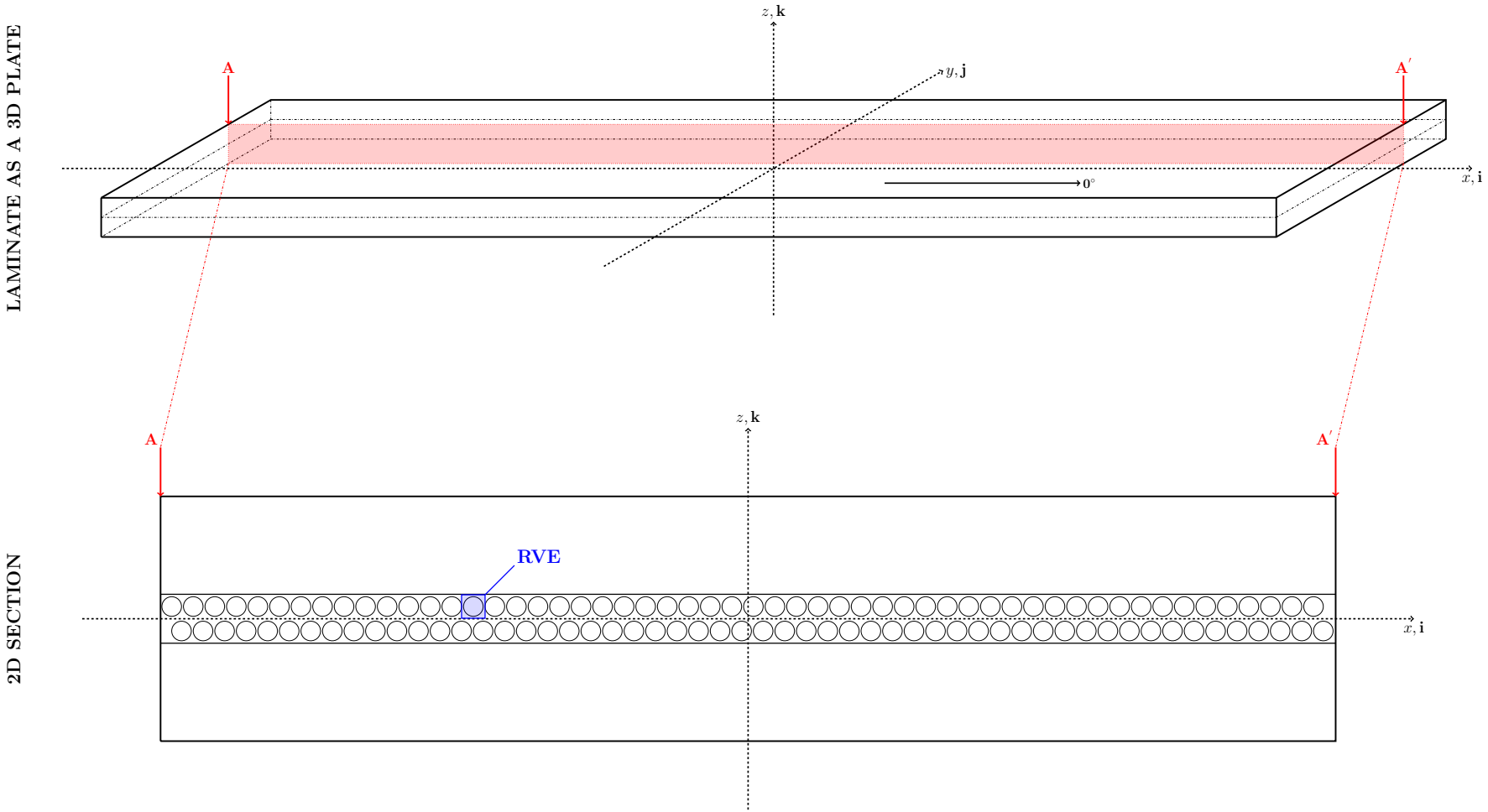

Representative Volume Elements (RVEs)

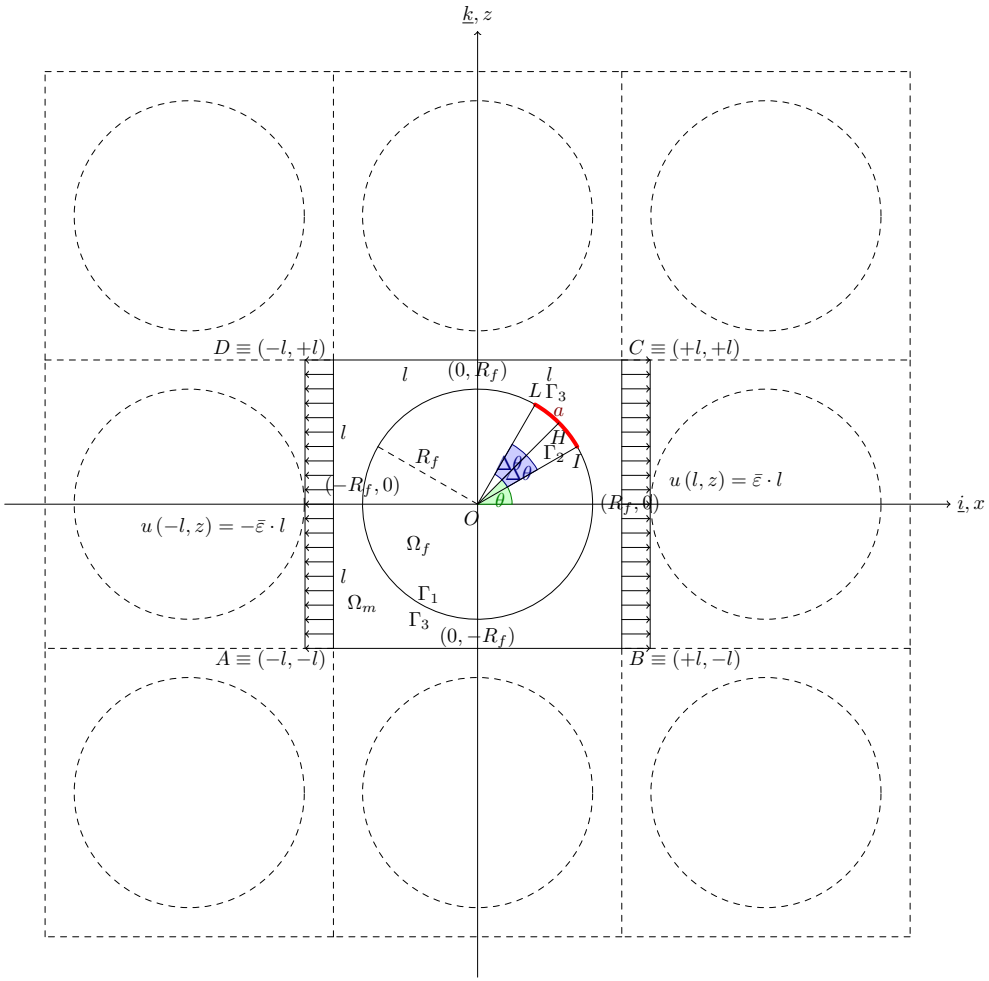

- ✓ 2D space
- ✓ Linear elastic materials
- ✓ Displacement control
- ✓ Dirichlet-type boundary conditions
- ✓ Linear elastic fracture mechanics
- ✓ Contact interaction

Mesh Design and Generation

Why a good mesh is fundamental

1. Geometric discretization has a strong effect on non-linear FEM simulations
2. Damage is a process that implies changes in geometry, i.e. generation of surfaces and domain splitting
3. Fracture mechanics quantities depends on the local mesh topology and refinement

4-step procedure for mesh generation

1. The boundary is generated patching analytical parameterizations
2. The boundary is split into a set of 4 corners (c_i) and 4 edges (e_i)
3. Interior nodes are created applying transfinite interpolation using multi-dimensional linear Lagrangian interpolants

$$P_1(x, p_j) = \sum_{j=1}^{n} p_j \prod_{k=1\ k\neq j}^{n} \frac{x - x_k}{x_j - x_k} \qquad P_2(x, y, p_j, q_j) = P_1(x, p_j) \otimes P_1(y, q_j)$$

$$r(\xi, \eta) = P_1(\xi, e_2, e_4) + P_1(\eta, e_1, e_3) - P_2(\xi, \eta, c_1, c_2, c_3, c_4)$$

4. The mesh is smoothed applying elliptic mesh generation

$$g^{11}\underline{r}_{,\xi\xi} + 2g^{12}\underline{r}_{,\xi\eta} + g^{22}\underline{r}_{,\eta\eta} = 0$$

Angular discretization

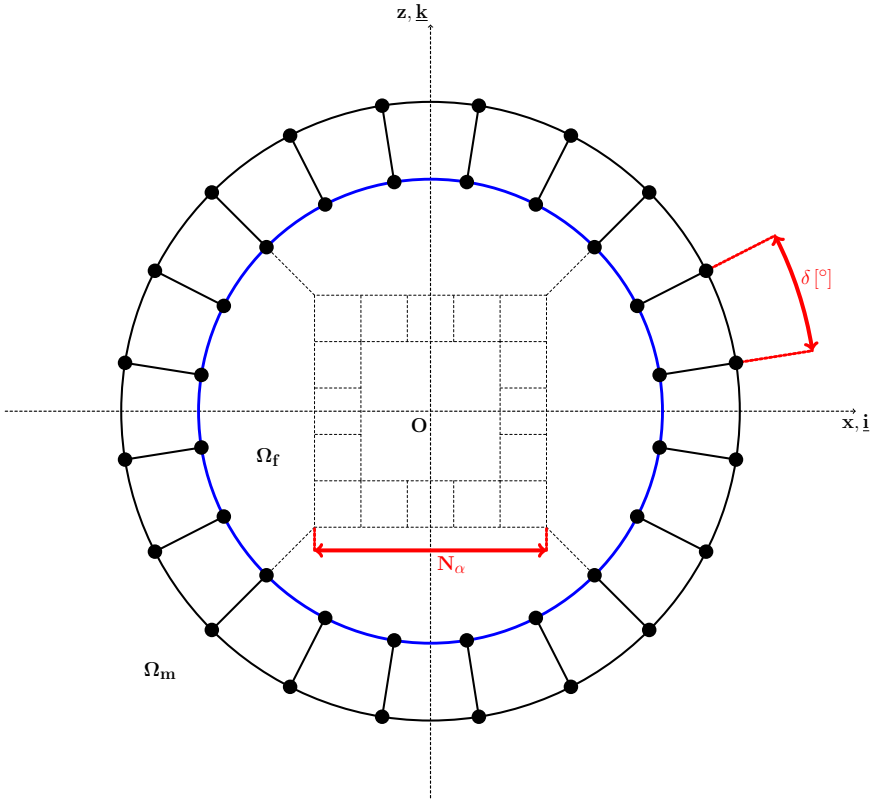

Angular discretization at fiber/matrix interface: $\delta = \frac{360^\circ}{4N_\alpha}$.

Virtual Crack Closure Technique (VCCT)

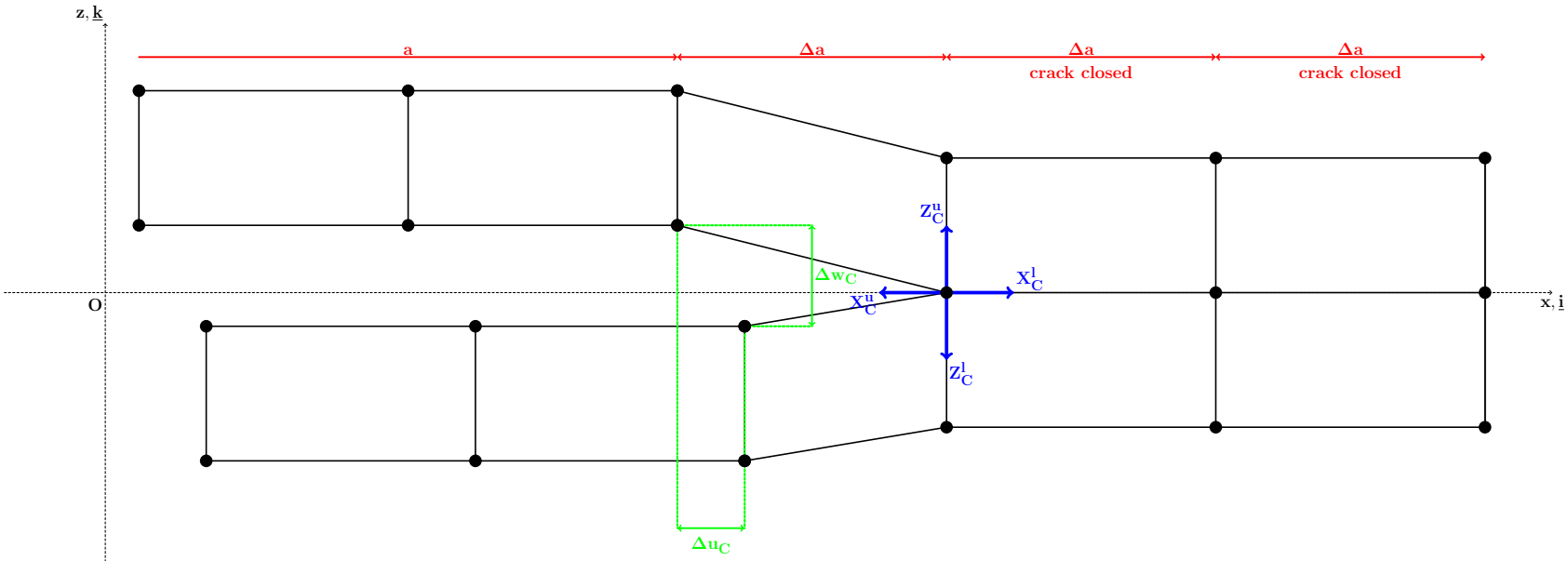

$$G_I = \frac{Z_C \Delta w_C}{2B\Delta a} \quad G_{II} = \frac{X_C \Delta u_C}{2B\Delta a} \iff \text{In-house routine and Abaqus}$$

J-integral evaluation

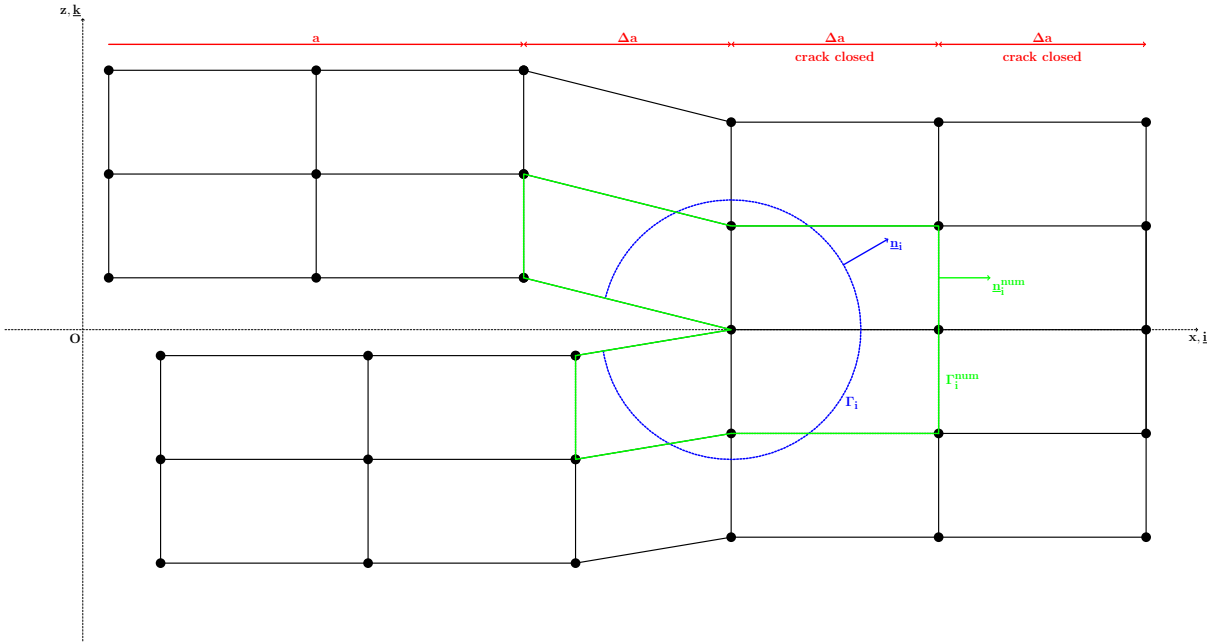

$$J_i = \lim_{\varepsilon \to 0} \int_{\Gamma_\varepsilon} \left(W(\Gamma)\, n_i - n_j \sigma_{jk} \frac{\partial u_k(\Gamma, x_i)}{\partial x_i} \right) d\Gamma \iff \text{*CONTOUR INTEGRAL in Abaqus}$$

↘ RESULTS

σ_0 for $Vf_f = 0.001$, $\frac{L}{R_f} \sim 28$ and $\delta = 0.4°$

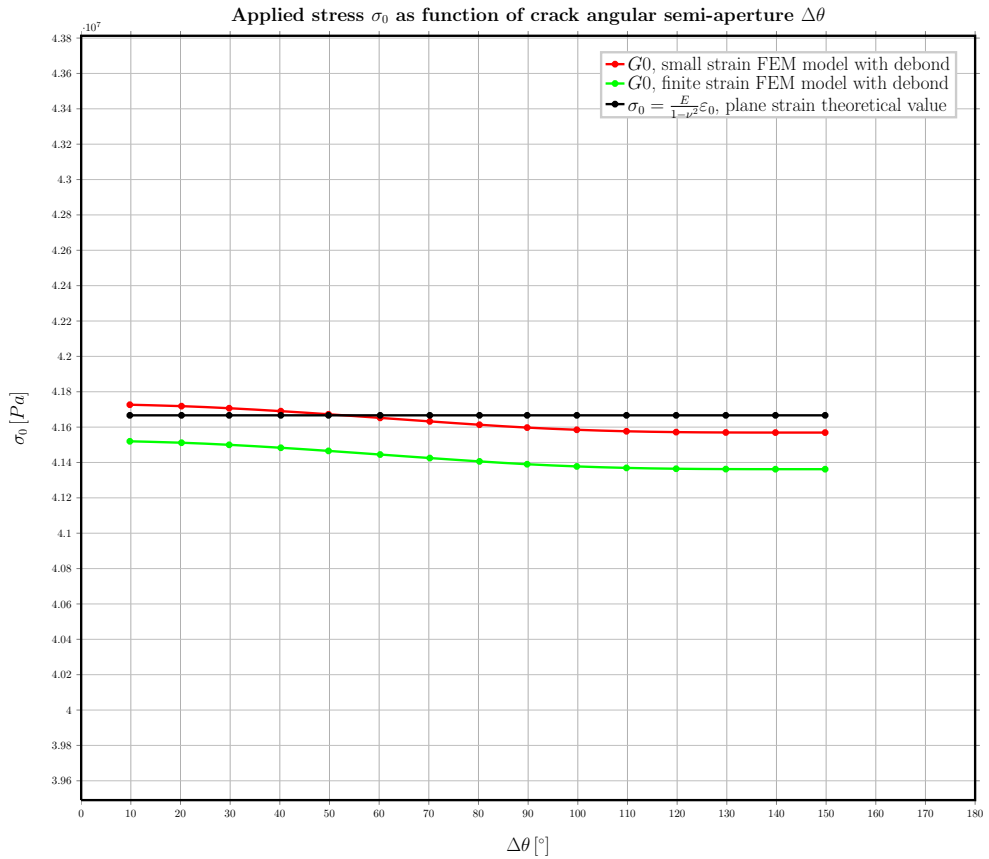

In red small strain FEM, in green finite strain FEM, in black $\sigma_0 = \frac{E}{1-\nu^2}\varepsilon$.

G_0 for $Vf_f = 0.001$, $\frac{L}{R_f} \sim 28$ and $\delta = 0.4°$

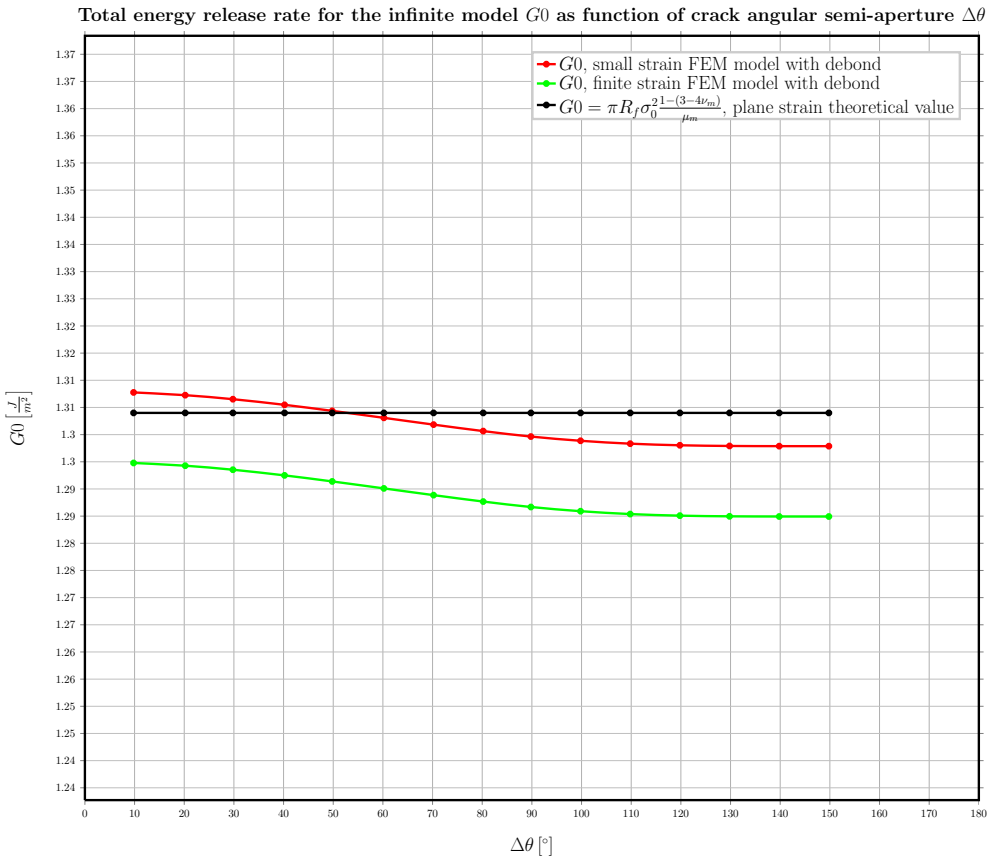

In red small strain FEM, in green finite strain FEM, in black G_0 calculated assuming $\sigma_0 = \frac{E}{1-\nu^2}\varepsilon$.

σ_0 **for** $Vf_f = 0.000079$, $\frac{L}{R_f} \sim 100$ **and** $\delta = 0.4°$

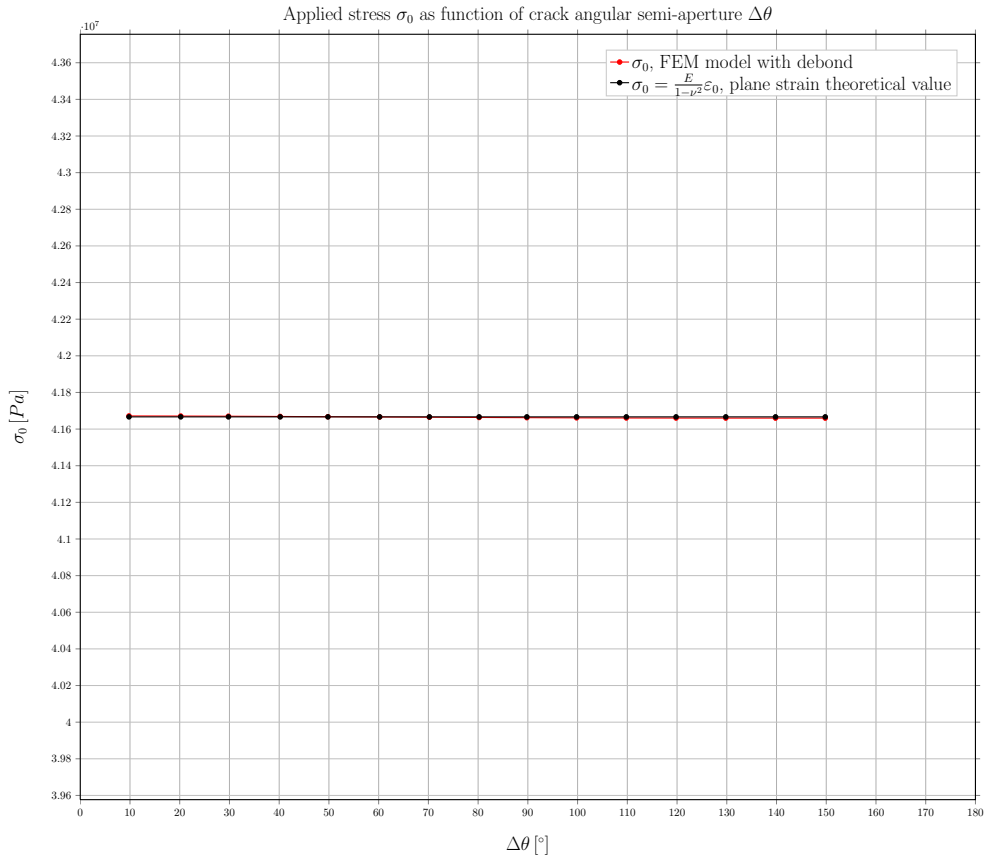

In red small strain FEM, in black $\sigma_0 = \frac{E}{1-\nu^2}\varepsilon$.

G_0 for $Vf_f = 0.000079$, $\frac{L}{R_f} \sim 100$ and $\delta = 0.4°$

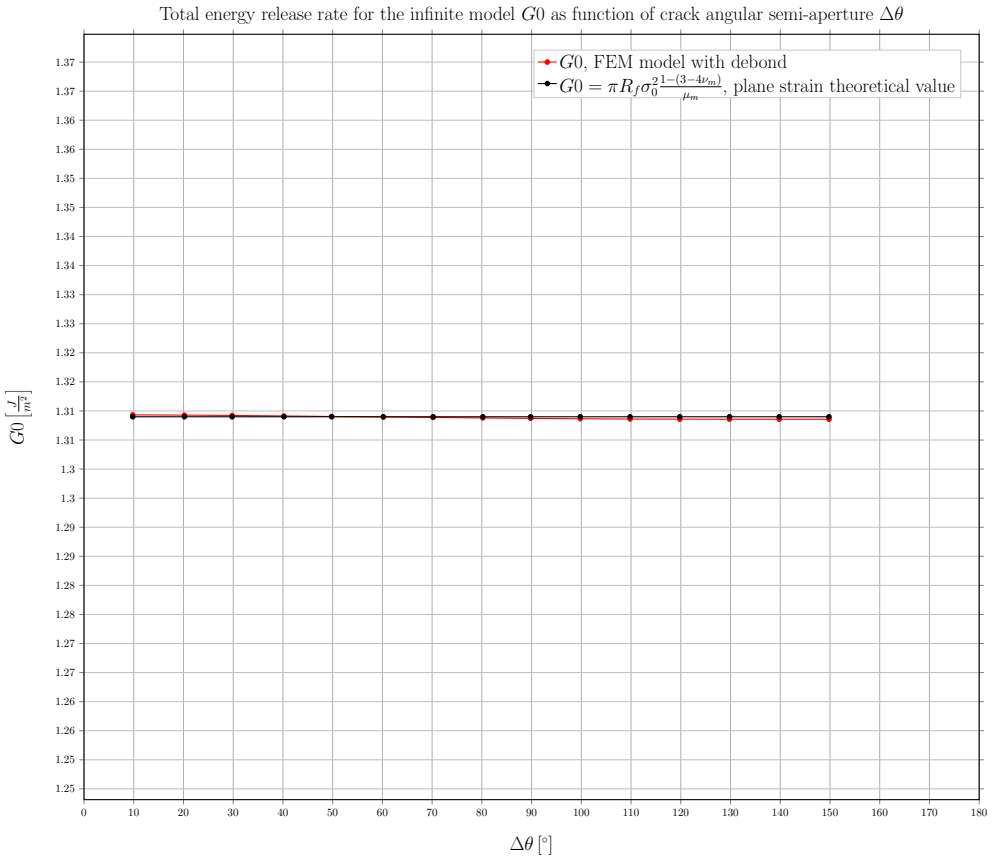

In red small strain FEM, in black G_0 calculated assuming $\sigma_0 = \frac{E}{1-\nu^2}\varepsilon$.

$\frac{G_{(..)}}{G_0}$ for $V_f = 0.001$, $\frac{L}{R_f} \sim 28$ and $\delta = 0.4°$

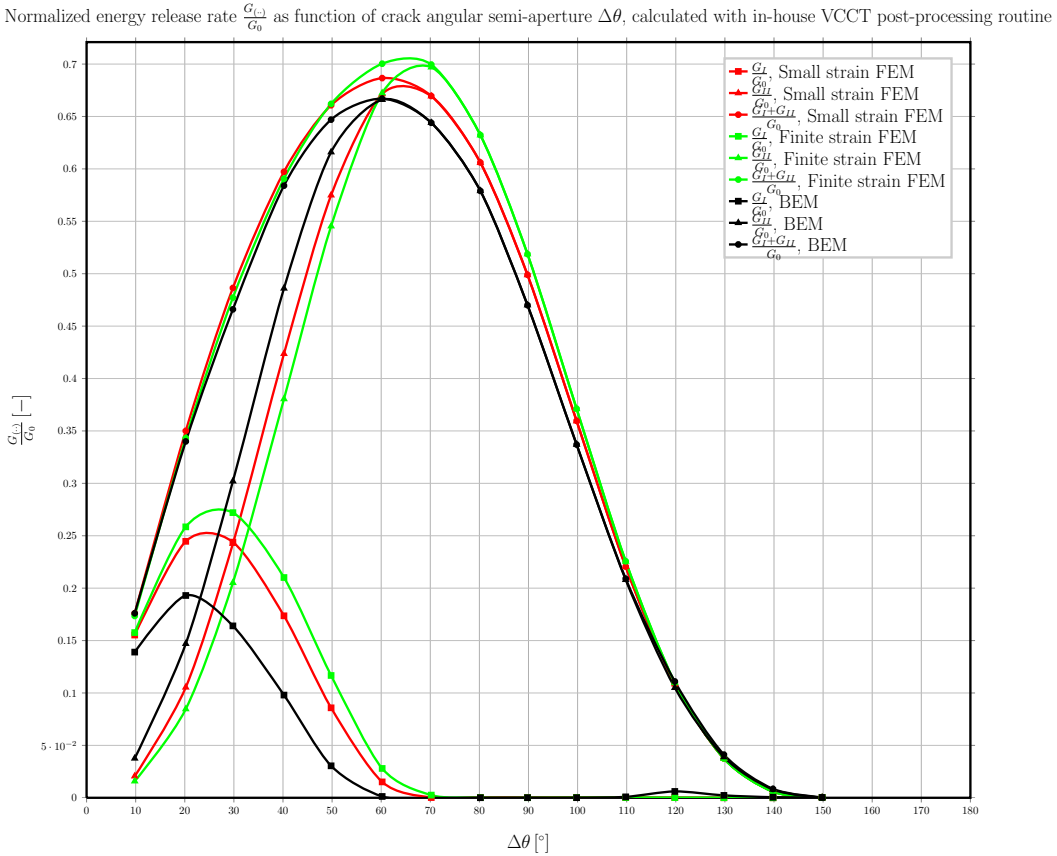

In red small strain FEM, in green finite strain FEM, in black BEM results.

$\frac{G_{(..)}}{G_0}$ for $V_f = 0.001$, $\frac{L}{R_f} \sim 28$ and $\delta = 0.4°$, small strain formulation

Normalized total energy release rate $\frac{G_{TOT}}{G_0}$ as function of crack angular semi-aperture $\Delta\theta$, calculated with Abaqus built-in J-Integral post-processing routine (*CONTOUR INTEGRAL)

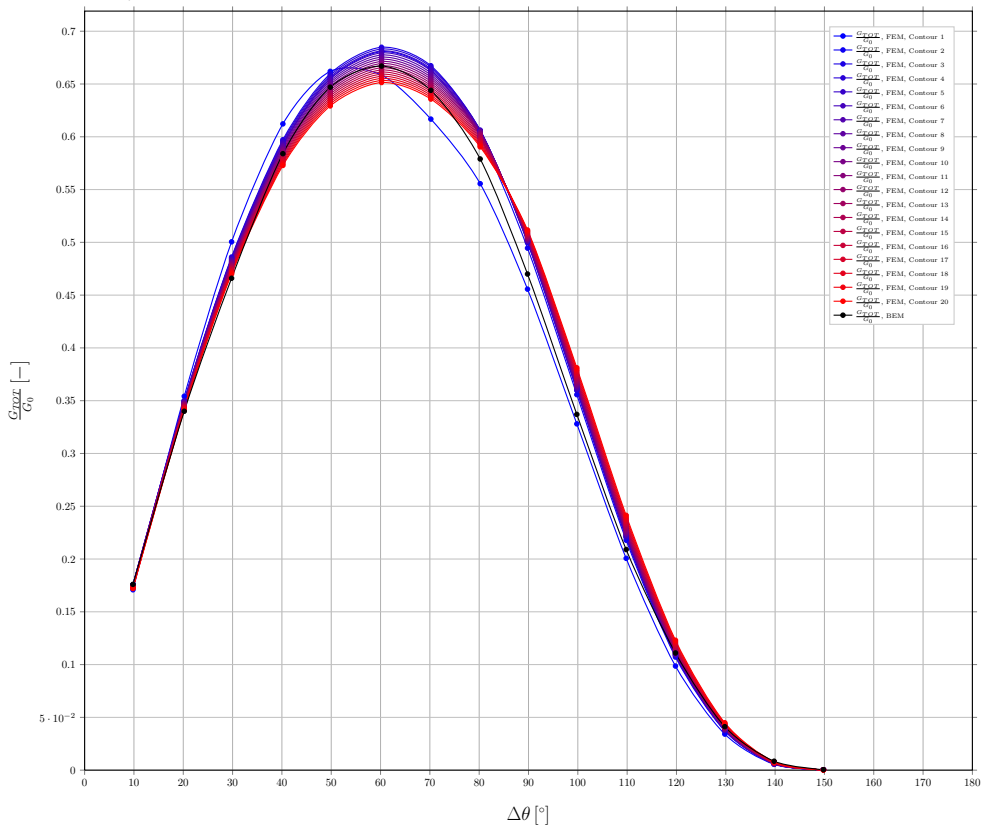

Fading from blue to red J-Integrals evaluated at contours at increasing distance from the crack tip, in black BEM results.

$\frac{G_{(..)}}{G_0}$ for $V_f = 0.001$, $\frac{L}{R_f} \sim 28$ and $\delta = 0.4°$, small strain formulation

Normalized energy release rate $\frac{G_{(..)}}{G_0}$ as function of crack angular semi-aperture $\Delta\theta$, calculated with in-house VCCT and Abaqus built-in J-Integral (*CONTOUR INTEGRAL) post-processing routines

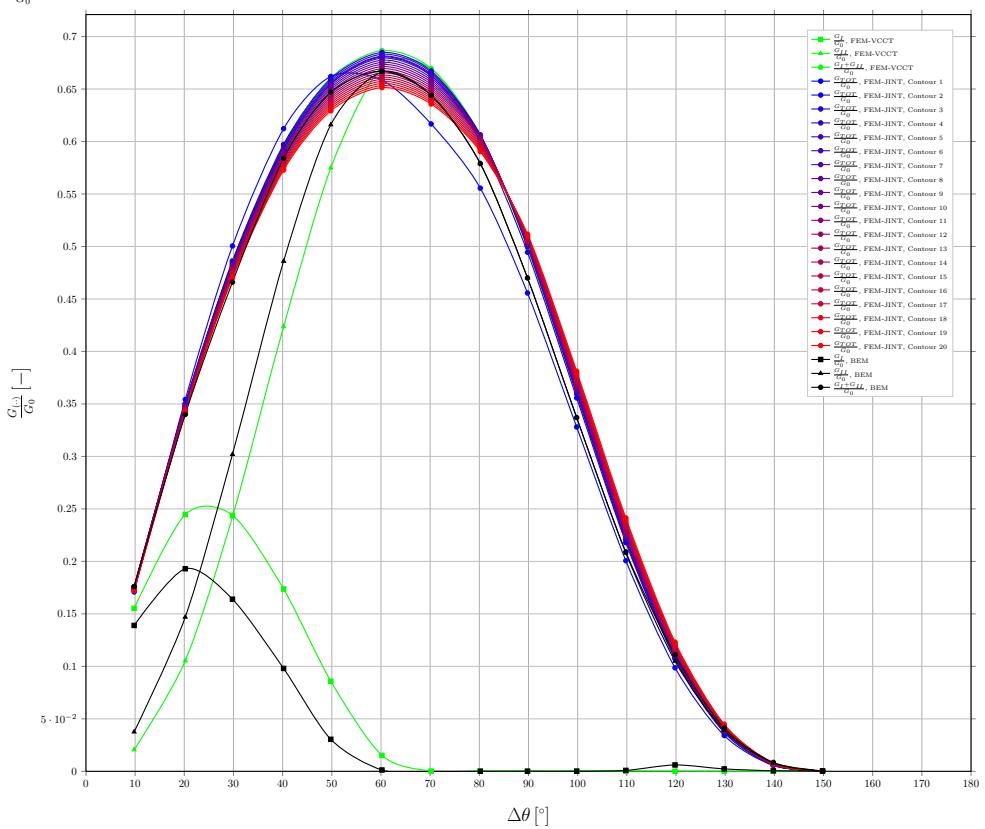

Fading from blue to red J-Integrals evaluated at contours at increasing distance from the crack tip, in green evaluation with in-house VCCT routine, in black BEM results.

$\frac{G_{(..)}}{G_0}$ for $V_f = 0.001$, $\frac{L}{R_f} \sim 28$ and $\delta = 0.4°$, finite strain formulation

Normalized total energy release rate $\frac{G_{TOT}}{G_0}$ as function of crack angular semi-aperture $\Delta\theta$, calculated with Abaqus built-in J-Integral post-processing routine (*CONTOUR INTEGRAL)

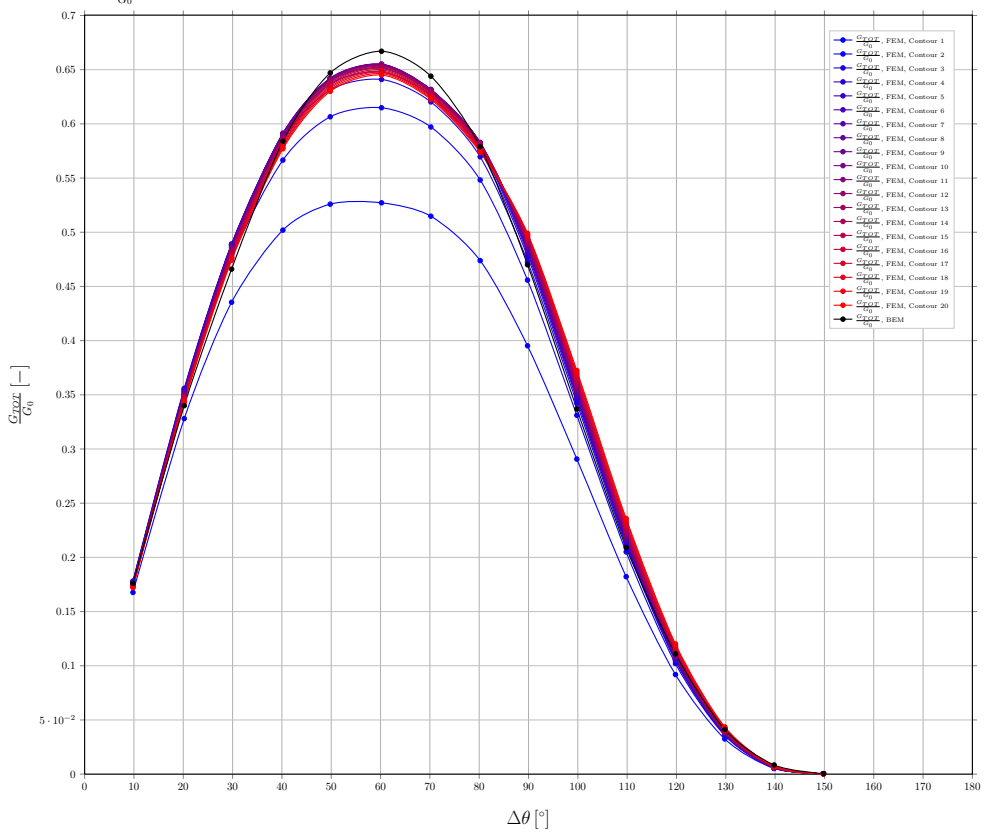

Fading from blue to red J-Integrals evaluated at contours at increasing distance from the crack tip, in black BEM results.

$\frac{G_{(..)}}{G_0}$ for $V_f = 0.001$, $\frac{L}{R_f} \sim 28$ and $\delta = 0.4°$, finite strain formulation

Normalized energy release rate $\frac{G_{(..)}}{G_0}$ as function of crack angular semi-aperture $\Delta\theta$, calculated with in-house VCCT and Abaqus built-in J-Integral (*CONTOUR INTEGRAL) post-processing routines

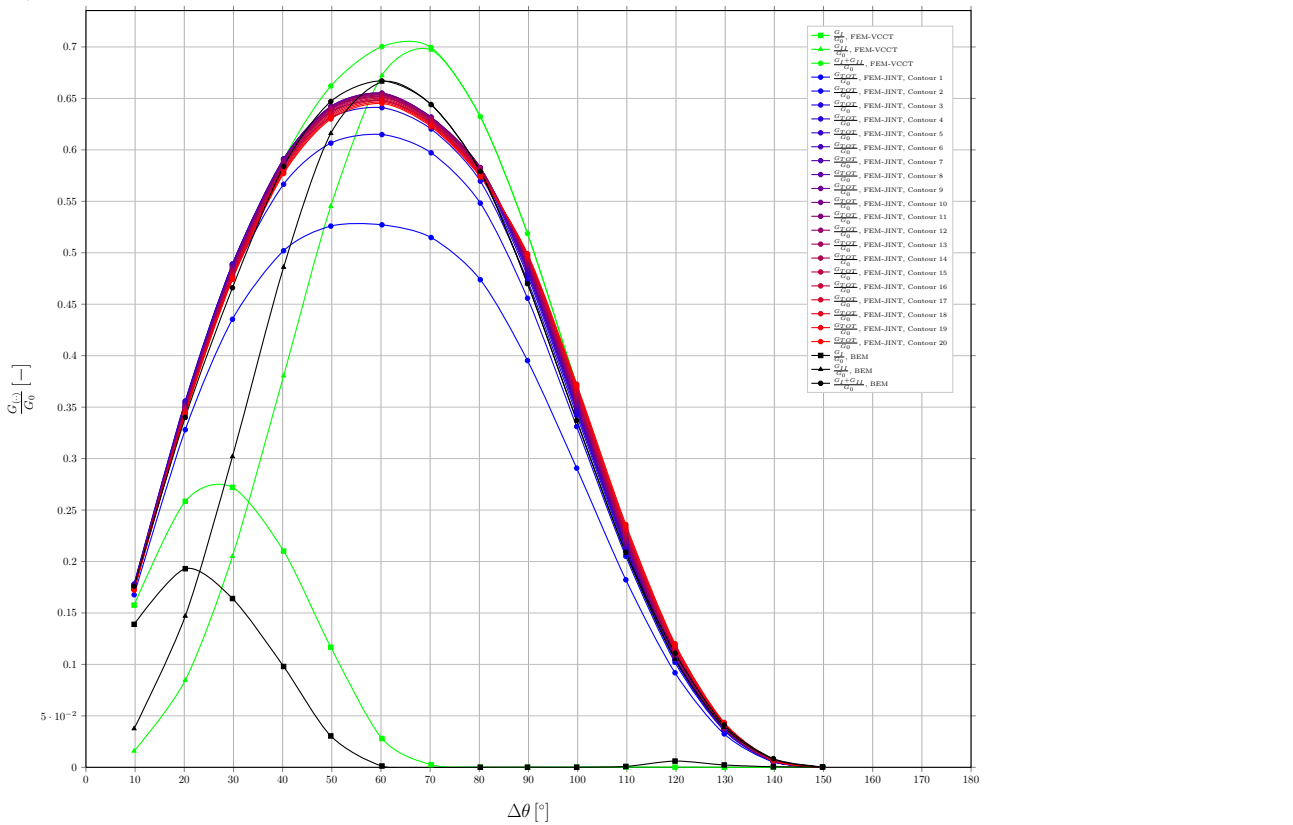

Fading from blue to red J-Integrals evaluated at contours at increasing distance from the crack tip, in green evaluation with in-house VCCT routine, in black BEM results.

CONCLUSIONS

Conclusions & Outlook

Conclusions

- 2D micromechanical models have been developed to investigate crack initiation in thin ply laminates
- A numerical procedure has been devised and implemented to automatize the creation of FEM models
- Analyses for $VF_f \rightarrow 0$ (matrix dominated RVE) conducted to validate the model with respect to previous literature

Outlook

- Investigate the dependence on VF_f, t_{ply}, $\frac{t_{ply}}{t_{bounding\ plies}}$ and different material systems
- Study numerical performances with respect to model's parameters
- Repeat for different RVEs and compare

APPENDICES & REFERENCES

Spread Tow Technology: Implications

- Strong reduction in ply's thickness and weight
- Reduction in laminate's thickness and weight
- Higher fiber volume fraction and more homogeneous fiber distribution
- Ply thickness to fiber diameter ratio decreases of at least 1 order of magnitude, from > 100 to ≤ 10
- Increased load at damage onset and increased ultimate strength, in particular for transverse cracking

RVEs: Variations on a Theme

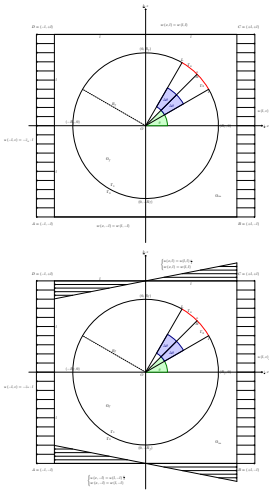

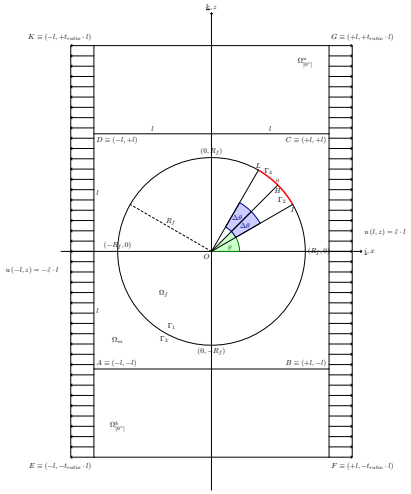

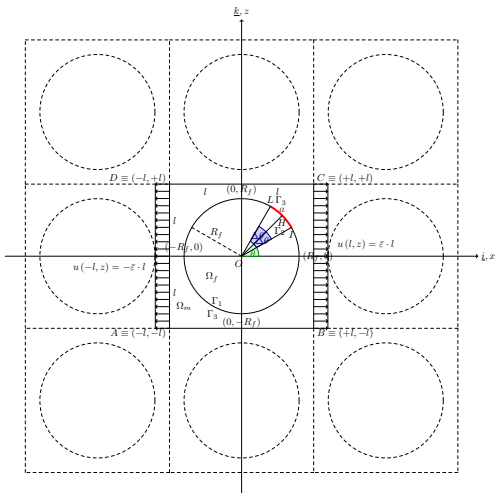

- ✓ 2D space
- ✓ Linear elastic materials
- ✓ Displacement control
- ✓ Dirichlet-type boundary conditions
- ✓ Linear elastic fracture mechanics
- ✓ Contact interaction

RVEs: First Variation on a Theme

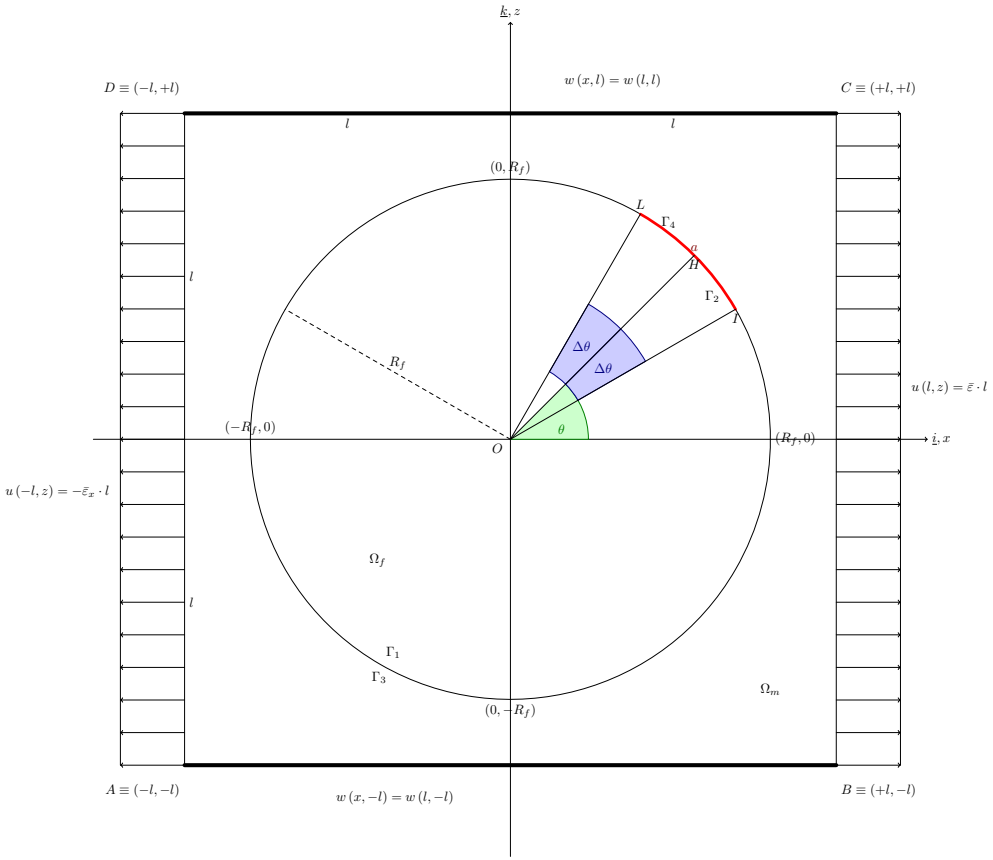

Isolated RVE with zero vertical displacement BC.

RVEs: Second Variation on a Theme

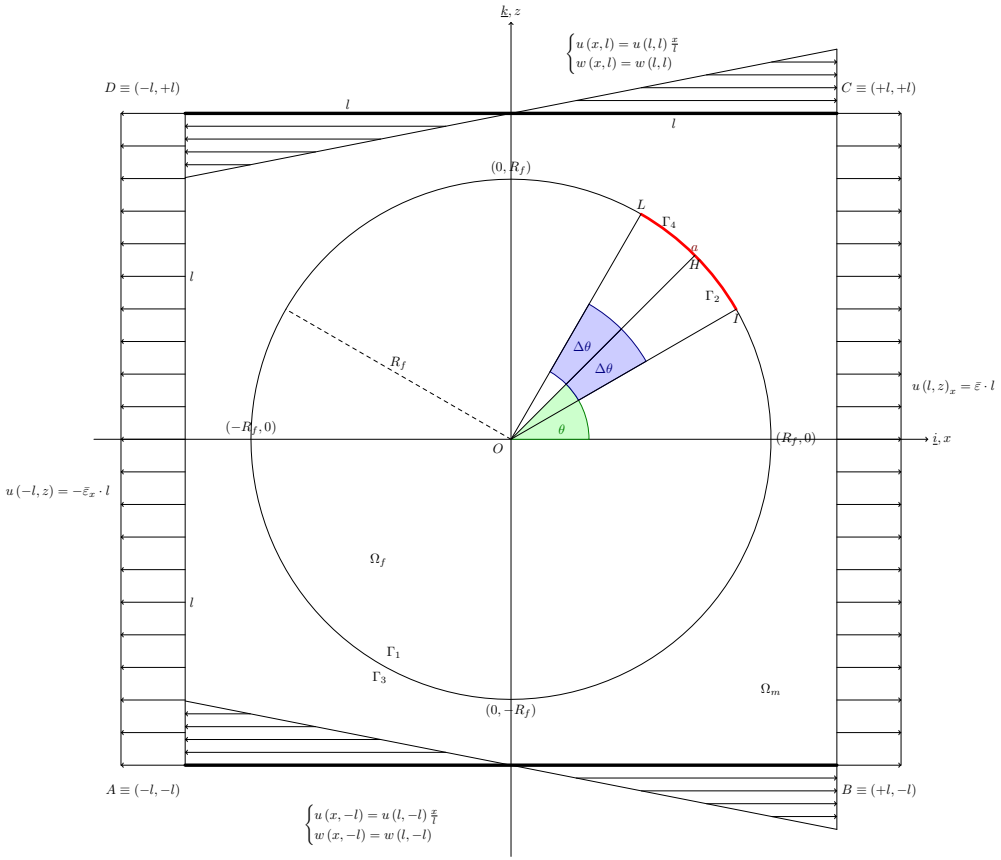

Isolated RVE with homogeneous displacement BC.

RVEs: Third Variation on a Theme

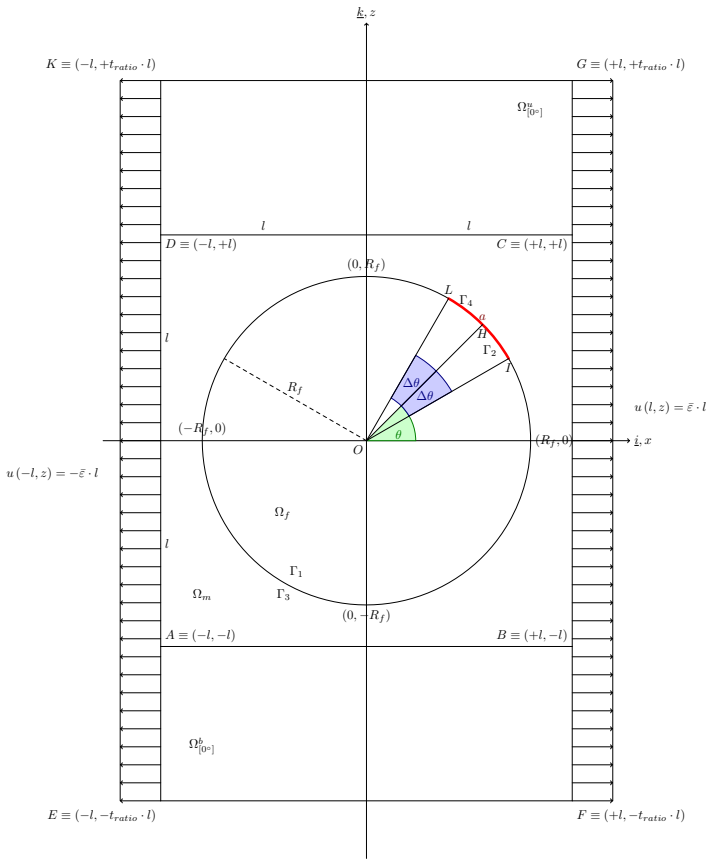

Bounded RVE.

Topological transformation

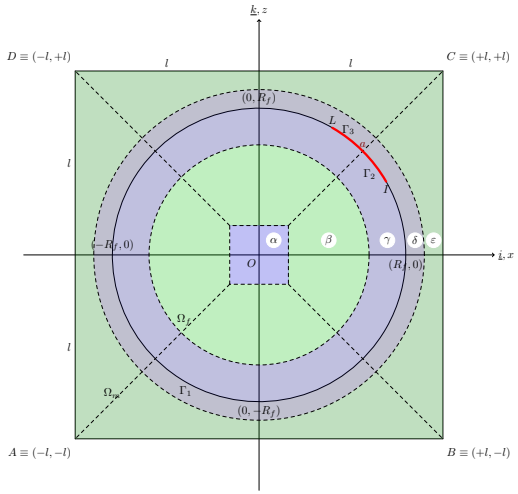

(a)

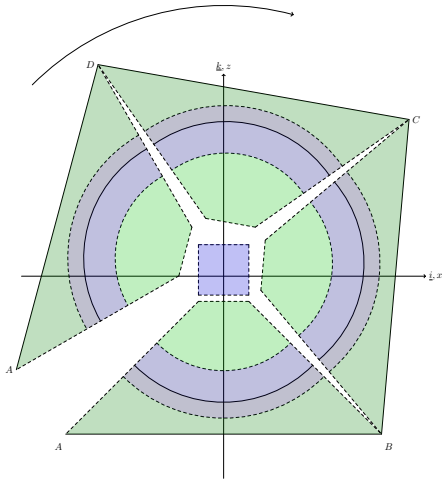

(b)

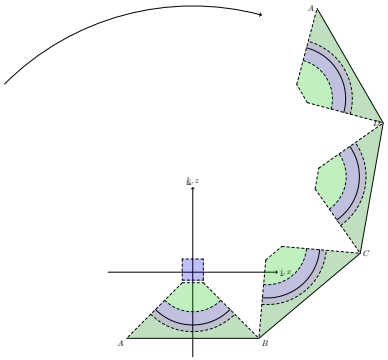

(c)

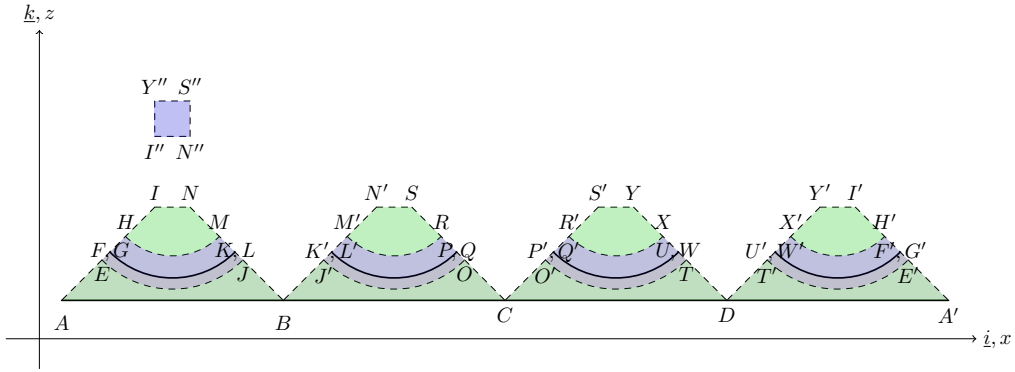

(d)

Mesh parameters

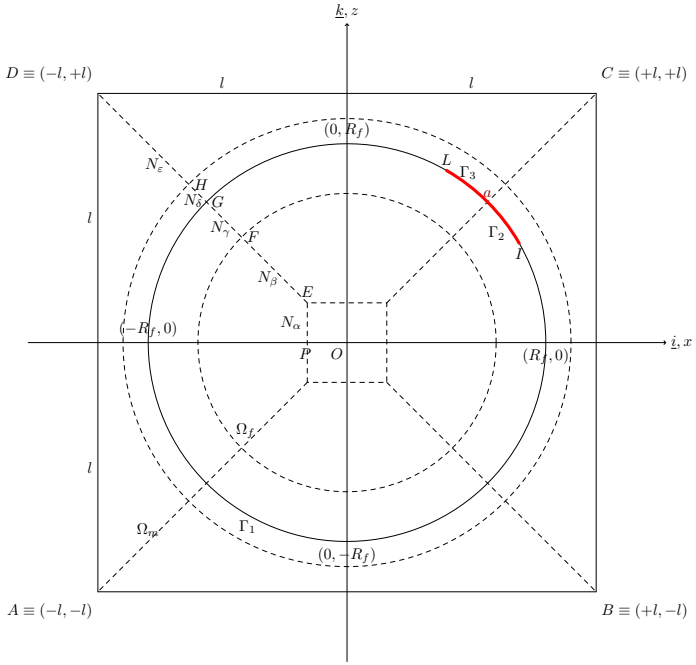

$E \equiv (-f_1 \cdot R_f, +f_1 \cdot R_f)$ $F \equiv f_2 R_f\,(-\cos 45°, \sin 45°)$

$G \equiv R_f\,(-\cos 45°, \sin 45°)$

$H \equiv (R_f + f_3\,(l - R_f))\,(-\cos 45°, \sin 45°)$

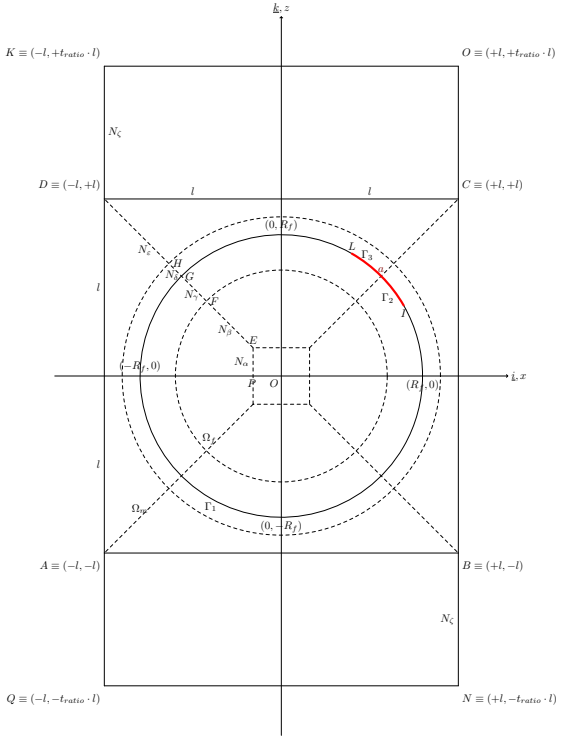

$E \equiv (-f_1 \cdot R_f, +f_1 \cdot R_f)$ $F \equiv f_2 R_f\,(-\cos 45°, \sin 45°)$

$G \equiv R_f\,(-\cos 45°, \sin 45°)$

$H \equiv (R_f + f_3\,(l - R_f))\,(-\cos 45°, \sin 45°)$

Finite Element Model in Abaqus

Method
ABAQUS/STD static analysis + VCCT + J-integral.

Type
Static, i.e. no inertial effects. Relaxation until equilibrium.

Elements
CPE4/CPE8

Interface
Tied surface constraint & contact mechanics

Input variables
R_f, V_f, material properties, interface properties.

Control variables
θ, $\Delta\theta$, $\bar{\varepsilon}_x$.

Output variables
Stress field, crack tip stress, stress intensity factors, energy release rates, a.

Evaluation of G_0

$$G_0 = \pi R_f \sigma_0^2 \frac{1 + k_m}{8 G_m} \tag{1}$$

$$k_m = 3 - 4\nu_m \tag{2}$$

$$\sigma_0^{undamaged} = \frac{E_m}{1 - \nu_m^2} \varepsilon_{xx} \tag{3}$$

References


Donald L. Flaggs, Murat H. Kural; *Experimental Determination of the In Situ Transverse Lamina Strength in Graphite/Epoxy Laminates.* Journal of Composite Materials, vol. 16, n. 2, 1982.


Parvizi A., Bailey J.E; *On multiple transverse cracking in glass fibre epoxy cross-ply laminates.* Journal of Materials Science, 1978; 13:2131-2136.

References

Miguel Herráez, Diego Mora, Fernando Naya, Claudio S. Lopes, Carlos González, Javier LLorca; *Transverse cracking of cross-ply laminates: A computational micromechanics perspective.* Composites Science and Technology, 2015; 110:196-204.

Luis Pablo Canal, Carlos González, Javier Segurado, Javier LLorca; *Intraply fracture of fiber-reinforced composites: Microscopic mechanisms and modeling.* Composites Science and Technology, 2012; 72(11):1223-1232.

References


Stephen W. Tsai; *Thin ply composites.* JEC Magazine 18, 2005.


Znedek P. Bazant; *Size Effect Theory and its Application to Fracture of Fiber Composites and Sandwich Plates.* in Continuum Damage Mechanics of Materials and Structures, eds. O. Allix and F. Hild, 2002.


Robin Amacher, Wayne Smith, Clemens Dransfeld, John Botsis, Joël Cugnoni; *Thin Ply: from Size-Effect Characterization to Real Life Design* CAMX 2014, 2014


Ralf Cuntze; *The World-Wide-Failure-Exercises -I and - II for UD-materials.*

References

Pinho, S. T. and Pimenta, S.; *Size Effects on the Strength and Toughness of Fibre-Reinforced Composites.*

Pedro P. Camanho, Carlos G. Dávila, Silvestre T. Pinho, Lorenzo Iannucci, Paul Robinson; *Prediction of in situ strengths and matrix cracking in composites under transverse tension and in-plane shear.* Composites Part A: Applied Science and Manufacturing, vol. 37, n. 2, 2006.

References

- P.P. Camanho, P. Maimí, C.G. Dávila; *Prediction of size effects in notched laminates using continuum damage mechanics.* Composites Science and Technology, vol. 67, n. 13, 2007.
- J. A. Nairn; *The Initiation and Growth of Delaminations Induced by Matrix Microcracks in Laminated Composites.* International Journal of Fracture, vol. 57, 1992.
- Joel Cugnoni , Robin Amacher, John Botsis; *Thin ply technology advantages. An overview of the TPT-TECA project.* 2014.

References

Donald L. Flaggs, Murat H. Kural; *Experimental Determination of the In Situ Transverse Lamina Strength in Graphite/Epoxy Laminates.* Journal of Composite Materials, vol. 16, n. 2, 1982.


Doc
MASE
UNIVERSITÉ
DE LORRAINE
EEIGM
LULEÅ
UNIVERSITY
OF TECHNOLOGY
Education and Culture
Erasmus Mundus